# COPYRIGHT NOTICE

The following document is subject to copyright agreements.

The attached copy is provided for your personal use on the understanding that you will not distribute it and that you will not include it in other published documents.

# Practical estimates of rock mass strength

E. Hoek and E.T. Brown

# Practical estimates of rock mass strength

E. HOEK[✦]
E.T. BROWN[✦✦]

The Hoek-Brown failure criterion was originally developed for estimating the strengths of hard rock masses. Because of the lack of suitable alternatives, the criterion has been applied to a variety of rock masses including very poor quality rocks, which could almost be classed as engineering soils. These applications have necessitated changes to the original criterion. One of the principal problems has been the determination of equivalent cohesive strengths and friction angles to meet the demands of software written in terms of the Mohr-Coulomb failure criterion. This paper summarises the interpretation of the Hoek-Brown failure criterion which has been found to work best in dealing with practical engineering problems.

## INTRODUCTION

Since its introduction in 1980 [1], the Hoek-Brown failure criterion has evolved to meet the needs of users who have applied it to conditions which were not visualised when it was originally developed. In particular, the increasing number of applications to very poor quality rock masses has necessitated some significant changes. The key equations involved in each of the successive changes are summarised in Appendix A.

The criterion is purely empirical and hence there are no 'correct' ways to interpret the various relationships which can be derived. Under the circumstances, it is not surprising that there have been a few less than useful mutations and that some users have been confused by the alternative interpretations which have been published.

This paper is an attempt to set the record straight and to present an interpretation of the criterion which covers the complete range of rock mass types and which has been found to work well in practice.

## GENERALISED HOEK-BROWN CRITERION

The Generalised Hoek-Brown failure criterion for jointed rock masses is defined by:

$$\sigma_1^{'} = \sigma_3^{'} + \sigma_{ci}\left( m_b \frac{\sigma_3^{'}}{\sigma_{ci}} + s \right)^a \qquad (1)$$

✦  Evert Hoek Consulting Engineer Inc.
   P.O. Box 75516, North Vancouver
   British Columbia, Canada, V7R 4X1
✦✦ Senior Deputy Vice Chancellor
   The University of Queensland
   Brisbane, Queensland 4072, Australia

where $\sigma_1^{'}$ and $\sigma_3^{'}$ are the maximum and minimum effective stresses at failure respectively,
$m_b$ is the value of the Hoek-Brown constant m for the rock mass,
s and a are constants which depend upon the characteristics of the rock mass, and
$\sigma_{ci}$ is the uniaxial compressive strength of the intact rock pieces.

It is possible to derive some exact mathematical relationships between the Hoek-Brown criterion, expressed in terms of the major and minor principal stresses, and the Mohr envelope, relating normal and shear stresses. However, these relationships are cumbersome and the original approach used by Hoek and Brown [1] is more practical. In this approach, equation (1) is used to generate a series of triaxial test values, simulating full scale field tests, and a statistical curve fitting process is used to derive an equivalent Mohr envelope defined by the equation:

$$\tau = A\sigma_{ci}\left( \frac{\sigma_n^{'} - \sigma_{tm}}{\sigma_{ci}} \right)^B \qquad (2)$$

where A and B are material constants
$\sigma_n^{'}$ is the normal effective stress, and
$\sigma_{tm}$ is the 'tensile' strength of the rock mass.

This 'tensile' strength, which reflects the interlocking of the rock particles when they are not free to dilate, is given by:

$$\sigma_{tm} = \frac{\sigma_{ci}}{2}\left( m_b - \sqrt{m_b^2 + 4s} \right) \qquad (3)$$

In order to use the Hoek-Brown criterion for estimating the strength and deformability of jointed rock masses, three 'properties' of the rock mass have to be estimated. These are

1. the uniaxial compressive strength $\sigma_{ci}$ of the intact rock pieces in the rock mass,
2. the value of the Hoek-Brown constant $m_i$ for these intact rock pieces, and
3. the value of the Geological Strength Index GSI for the rock mass.

## THE EFFECT OF WATER

Many rocks show a significant strength decrease with increasing moisture content. In some cases, such as montmorillonitic clay shales, saturation destroys the specimens completely. More typically, strength losses of 30 to100 % occur in many rocks as a result of chemical deterioration of the cement or clay binder (Broch [2]). Samples which have been left to dry in a core shed for several months, can give a misleading impression of the rock strength. Laboratory tests should be carried out at moisture contents which are as close as possible to those which occur in the field.

A more important effect is the strength reduction which occurs as a result of water pressures in the pore spaces in the rock. Terzaghi [3] formulated the concept of effective stress for porous media such as soils. The effective stress 'law', as it is frequently called, can be expressed as $\sigma' = \sigma - u$ where $\sigma'$ is the effective or intergranular stress which controls the strength and the deformation of the material, $\sigma$ is the total stress applied to the specimen and $u$ is the pore water pressure. In a comprehensive review of the applicability of the effective stress concept to soil, concrete and rock, Lade and de Boer [4] conclude that the relationship proposed by Terzaghi works well for stress magnitudes encountered in most geotechnical applications, but that significant deviations can occur at very high stress levels.

The effective stress principle has been used throughout this paper for both intact rock and jointed rock masses. For intact rocks, with very low porosity, it has been assumed that stress changes are slow enough for the pore pressures in the rock specimens to reach steady state conditions (Brace and Martin [5]). In jointed rock masses, it may be expected that the water pressures in the discontinuities will build up and dissipate more rapidly than those in the pores of the intact rock blocks, especially in low porosity and permeability rocks. For this reason, a distinction is sometimes made between joint and pore water pressures in jointed rock masses. When applying the Hoek - Brown criterion to heavily jointed rock masses, isotropic behaviour involving failure on the discontinuities is assumed. In these cases, the water or 'pore' pressures governing the effective stresses will be those generated in the interconnected discontinuities defining the particles in an equivalent isotropic medium.

In applying the failure criterion, expressed in effective stress terms, to practical design problems it is necessary to determine the pore pressure distribution in the rock mass being analysed. This can be done by direct measurement, using piezometers, or estimated from manually constructed or numerically generated flow nets. In the case of slopes, dam foundations and tunnels subjected to fluctuating internal water pressure, the magnitude of the pore pressures can be of the same order as the induced rock stresses and hence it is very important to deal with the analysis in terms of effective stresses. In other cases, particularly when designing under-ground excavations, it can be assumed that the rock mass surrounding these excavations will be fully drained and hence the pore pressures are set to zero.

## INTACT ROCK PROPERTIES

For the intact rock pieces that make up the rock mass equation (1) simplifies to:

$$\sigma'_1 = \sigma'_3 + \sigma_{ci}\left(m_i \frac{\sigma'_3}{\sigma_{ci}} + 1\right)^{0.5} \qquad (4)$$

The relationship between the effective principal stresses at failure for a given rock is defined by two constants, the uniaxial compressive strength $\sigma_{ci}$ and a constant $m_i$. Wherever possible the values of these constants should be determined by statistical analysis of the results of a set of triaxial tests on carefully prepared core samples, as described in Appendix B.

Note that the range of minor principal stress ($\sigma'_3$) values over which these tests are carried out is critical in determining reliable values for the two constants. In deriving the original values of $\sigma_{ci}$ and $m_i$, Hoek and Brown [1] used a range of $0 < \sigma'_3 < 0.5\sigma_{ci}$ and, in order to be consistent, it is essential that the same range be used in any laboratory triaxial tests on intact rock specimens.

When laboratory tests are not possible, Tables 1 and 2 can be used to obtain estimates of $\sigma_{ci}$ and $m_i$. These estimates can be used for preliminary design purposes but, for detailed design studies, laboratory tests should be carried out to obtain values that are more reliable.

When testing very hard brittle rocks it may be worth considering the fact that short-term laboratory tests tend to overestimate the in-situ rock mass strength. Extensive laboratory tests and field studies on excellent quality Lac du Bonnet granite, reported by Martin and Chandler [7], suggest that the in-situ strength of this rock is only about 70% of that measured in the laboratory. This appears to be due to

the fact that damage resulting from micro-cracking of the rock initiates and develops critical intensities at lower stress levels in the field than in laboratory tests carried out at higher loading rates on smaller specimens.

Anisotropic and foliated rocks such as slates, schists and phyllites, whose behaviour is dominated by closely spaced planes of weakness, cleavage or schistosity, present particular difficulties in the determination of the uniaxial compressive strengths.

Salcedo [8] has reported the results of a set of directional uniaxial compressive tests on a graphitic phyllite from Venezuela. These results are summarised in Fig. 1. It will be noted that the uniaxial compressive strength of this material varies by a factor of about 5, depending upon the direction of loading. Evidence of the behaviour of this graphitic phyllite in the field suggests that the rock mass properties are dependent upon the strength parallel to schistosity rather than that normal to it.

In deciding upon the value of $\sigma_{ci}$ for foliated rocks, a decision has to be made on whether to use the highest or the lowest uniaxial compressive strength obtained from results such as those given in Fig. 1. Mineral composition, grain size, grade of metamorphism and tectonic history all play a role in determining the characteristics of the rock mass.

The authors cannot offer any precise guidance on the choice of $\sigma_{ci}$ but suggest that the maximum value should be used for hard, well interlocked rock masses such as good quality slates. The lowest uniaxial compressive strength should be used for tectonically disturbed, poor quality rock masses such as the graphitic phyllite tested by Salcedo [8].

Table 1. Field estimates of uniaxial compressive strength.

| Grade* | Term | Uniaxial Comp. Strength (MPa) | Point Load Index (MPa) | Field estimate of strength | Examples |
|---|---|---|---|---|---|
| R6 | Extremely Strong | > 250 | >10 | Specimen can only be chipped with a geological hammer | Fresh basalt, chert, diabase, gneiss, granite, quartzite |
| R5 | Very strong | 100 - 250 | 4 - 10 | Specimen requires many blows of a geological hammer to fracture it | Amphibolite, sandstone, basalt, gabbro, gneiss, granodiorite, limestone, marble, rhyolite, tuff |
| R4 | Strong | 50 - 100 | 2 - 4 | Specimen requires more than one blow of a geological hammer to fracture it | Limestone, marble, phyllite, sandstone, schist, shale |
| R3 | Medium strong | 25 - 50 | 1 - 2 | Cannot be scraped or peeled with a pocket knife, specimen can be fractured with a single blow from a geological hammer | Claystone, coal, concrete, schist, shale, siltstone |
| R2 | Weak | 5 - 25 | ** | Can be peeled with a pocket knife with difficulty, shallow indentation made by firm blow with point of a geological hammer | Chalk, rocksalt, potash |
| R1 | Very weak | 1 - 5 | ** | Crumbles under firm blows with point of a geological hammer, can be peeled by a pocket knife | Highly weathered or altered rock |
| R0 | Extremely weak | 0.25 - 1 | ** | Indented by thumbnail | Stiff fault gouge |

*  Grade according to Brown [2]
** Point load tests on rocks with a uniaxial compressive strength below 25 MPa are likely to yield ambiguous results.

Table 2. Values of the constant $m_i$ for intact rock, by rock group. Note that values in parenthesis are estimates.

| Rock type | Class | Group | Texture | | | |
|---|---|---|---|---|---|---|
| | | | Coarse | Medium | Fine | Very fine |
| SEDIMENTARY | Clastic | | Conglomerate (22) | Sandstone 19 | Siltstone 9 | Claystone 4 |
| | | | ——— Greywacke ——— (18) | | | |
| | Non-Clastic | Organic | ——— Chalk ——— 7 | | | |
| | | | ——— Coal ——— (8-21) | | | |
| | | Carbonate | Breccia (20) | Sparitic Limestone (10) | Micritic Limestone 8 | |
| | | Chemical | | Gypstone 16 | Anhydrite 13 | |
| METAMORPHIC | Non Foliated | | Marble 9 | Hornfels (19) | Quartzite 24 | |
| | Slightly foliated | | Migmatite (30) | Amphibolite 25 - 31 | Mylonites (6) | |
| | Foliated* | | Gneiss 33 | Schists 4 - 8 | Phyllites (10) | Slate 9 |
| IGNEOUS | Light | | Granite 33 | | Rhyolite (16) | Obsidian (19) |
| | | | Granodiorite (30) | | Dacite (17) | |
| | | | Diorite (28) | | Andesite 19 | |
| | Dark | | Gabbro 27 | Dolerite (19) | Basalt (17) | |
| | | | Norite 22 | | | |
| | Extrusive pyroclastic type | | Agglomerate (20) | Breccia (18) | Tuff (15) | |

* These values are for intact rock specimens tested normal to bedding or foliation. The value of $m_i$ will be significantly different if failure occurs along a weakness plane.

Unlike other rocks, coal is organic in origin and therefore has unique constituents and properties. Unless these properties are recognised and allowed for in characterising the coal, the results of any tests will exhibit a large amount of scatter. Medhurst, Brown and Trueman [9] have shown that, by taking into account the 'brightness' which reflects the composition and the cleating of the coal, it is possible to differentiate between the mechanical characteristics of different coals.

## INFLUENCE OF SAMPLE SIZE

The influence of sample size upon rock strength has been widely discussed in geotechnical literature and it is generally assumed that there is a significant reduction in strength with increasing sample size. Based upon an analysis of published data, Hoek and Brown [1] have suggested that the uniaxial compressive strength $\sigma_{cd}$ of a rock specimen with a diameter of d mm is related to the uniaxial

compressive strength $\sigma_{c50}$ of a 50 mm diameter sample by equation (5).

$$\sigma_{cd} = \sigma_{c50}\left(\frac{50}{d}\right)^{0.18} \qquad (5)$$

This relationship, together with the data upon which it was based, is illustrated in Fig. 2.

The authors suggest that the reduction in strength is due to the greater opportunity for failure through and around grains, the 'building blocks' of the intact rock, as more and more of these grains are included in the test sample. Eventually, when a sufficiently large number of grains are included in the sample, the strength reaches a constant value.

Medhurst and Brown [10] have reported the results of laboratory triaxial tests on samples of 61, 101, 146 and 300 mm diameter samples of a highly cleated mid-brightness coal from the Moura mine in Australia. The results of these tests are summarised in Table 3 and Fig. 3.

4 which shows the transition from an isotropic intact rock specimen, through a highly anisotropic rock mass in which failure is controlled by one or two discontinuities, to an isotropic heavily jointed rock mass.

The Hoek-Brown failure criterion, which assumes isotropic rock and rock mass behaviour, should only be applied to those rock masses in which there are a sufficient number of closely spaced discontinuities that isotropic behaviour involving failure on discontinuities can be assumed. Where the block size is of the same order as that of the structure being analysed, the Hoek-Brown criterion should not be used. The stability of the structure should be analysed by considering the behaviour of blocks and wedges defined by intersecting structural features. When the slope or underground excavation is large and the block size small in comparison, the rock mass can be treated as a Hoek-Brown material.
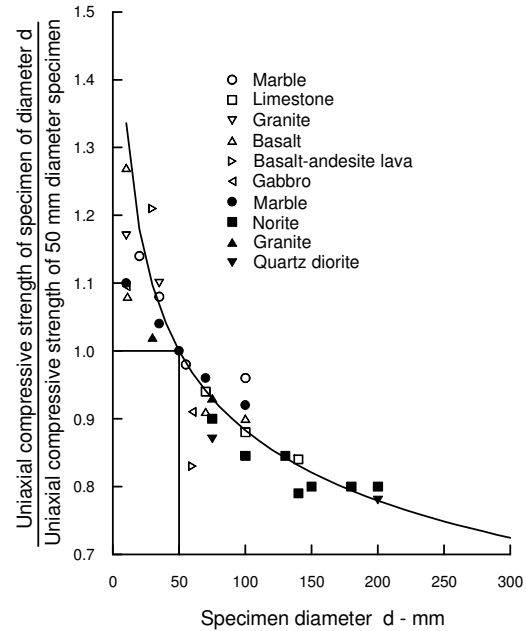


Fig. 1. Influence of loading direction on strength of graphitic phyllite tested by Salcedo [8].



Fig. 2. Influence of specimen size on the strength of intact rock. After Hoek and Brown [1].

The results obtained by Medhurst and Brown show a significant decrease in strength with increasing sample size. This is attributed to the effects of cleat spacing. For this coal, the persistent cleats are spaced at 0.3 to 1.0 m while non-persistent cleats within vitrain bands and individual lithotypes define blocks of 1 cm or less. This cleating results in a 'critical' sample size of about 1 m above which the strength remains constant.

It is reasonable to extend this argument further and to suggest that, when dealing with large scale rock masses, the strength will reach a constant value when the size of individual rock pieces is sufficiently small in relation to the overall size of the structure being considered. This suggestion is embodied in Fig.

Table 3. Peak strength of Moura DU coal in terms of the parameters contained in equation (1), based upon a value of $\sigma_{ci} = 32.7$ MPa.

| Dia.(mm) | $m_b$ | $s$ | $a$ |
|---|---|---|---|
| 61 | 19.4 | 1.0 | 0.5 |
| 101 | 13.3 | 0.555 | 0.5 |
| 146 | 10.0 | 0.236 | 0.5 |
| 300 | 5.7 | 0.184 | 0.6 |
| mass | 2.6 | 0.052 | 0.65 |
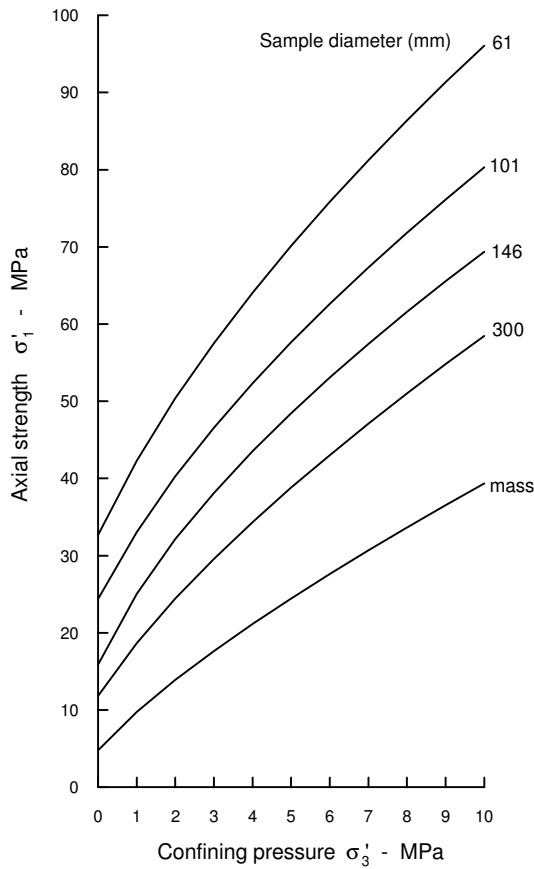
Fig. 3. Peak strength for Australian Moura coal. After Medhurst and Brown [6].
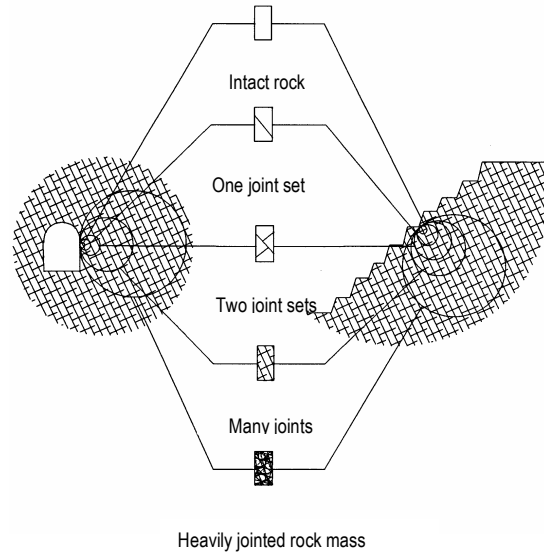


Fig. 4. Idealised diagram showing the transition from intact to a heavily jointed rock mass with increasing sample size.

Once the Geological Strength Index has been estimated, the parameters which describe the rock mass strength characteristics, are calculated as follows:

$$m_b = m_i \ \exp\left(\frac{GSI - 100}{28}\right) \qquad (6)$$

For GSI > 25, i.e. rock masses of good to reasonable quality, the original Hoek-Brown criterion is applicable with

$$s = \exp\left(\frac{GSI - 100}{9}\right) \qquad (7)$$

and

$$a = 0.5 \qquad (8)$$

For GSI < 25, i.e. rock masses of very poor quality, the modified Hoek-Brown criterion [14] applies with

$$s = 0 \qquad (9)$$

and

$$a = 0.65 - \frac{GSI}{200} \qquad (10)$$

The choice of GSI = 25 for the switch between the original and modified criteria is purely arbitrary. It could be argued that a switch at GSI = 30 would not introduce a discontinuity in the value of a, but extensive trials have shown that the exact location of this switch has negligible practical significance.

For better quality rock masses (GSI > 25), the value of GSI can be estimated directly from the 1976 version of Bieniawski's Rock Mass Rating, with the Groundwater rating set to 10 (dry) and the Adjustment for Joint Orientation set to 0 (very favourable) [15]. For very poor quality rock masses

## GEOLOGICAL STRENGTH INDEX

The strength of a jointed rock mass depends on the properties of the intact rock pieces and also upon the freedom of these pieces to slide and rotate under different stress conditions. This freedom is controlled by the geometrical shape of the intact rock pieces as well as the condition of the surfaces separating the pieces. Angular rock pieces with clean, rough discontinuity surfaces will result in a much stronger rock mass than one which contains rounded particles surrounded by weathered and altered material. The Geological Strength Index (GSI), introduced by Hoek [11] and Hoek, Kaiser and Bawden [12] provides a system for estimating the reduction in rock mass strength for different geological conditions. This system is presented in Tables 4 and 5. Experience has shown that Table 4 is sufficient for field observations since it is only necessary to note the letter code which identifies each rock mass category. These codes can then be used to estimate the GSI value from Table 5.

the value of RMR is very difficult to estimate and the balance between the ratings no longer gives a reliable basis for estimating rock mass strength. Consequently, Bieniawski's RMR classification should not be used for estimating the GSI values for poor quality rock masses.

If the 1989 version of Bieniawski's RMR classification [16] is used, then GSI = $RMR_{89}$' - 5 where $RMR_{89}$' has the Groundwater rating set to 15 and the Adjustment for Joint Orientation set to zero.

One of the practical problems which arises when assessing the value of GSI in the field is related to blast damage. As illustrated in Fig. 5, there is a considerable difference in the appearance of a rock face which has been excavated by controlled blasting and a face which has been damaged by bulk blasting. Wherever possible, the undamaged face should be used to estimate the value of GSI since the overall aim is to determine the properties of the undisturbed rock mass. Where all the visible faces have been damaged by blasting, some attempt should be made to compensate for the lower values of GSI obtained from such faces. In recently blasted faces, new discontinuity surfaces will have been created by the blast and these will give a GSI value which may be as much as 10 points lower than that for the undisturbed rock mass. In other words, severe blast damage can be allowed for by moving up one row in Tables 4 and 5. Where blast damaged faces have been exposed for a number of years, it may also be necessary to step as much as one column to the left in order to allow for surface weathering which will have occurred during this exposure. Hence, for example, a badly blast damaged weathered rock surface which has the appearance of a BLOCKY/DISTURBED and FAIR (BD/F in Table 4) rock mass may actually be VERY BLOCKY and GOOD (VB/G) in its unweathered and undisturbed in-situ state.

An additional practical question is whether borehole cores can be used to estimate the GSI value behind the visible faces? For reasonable quality rock masses (GSI > 25) the best approach is to evaluate the core in terms of Bieniawski's RMR classification and then, as described above, to estimate the GSI value from RMR. For poor quality rock masses (GSI < 25), relatively few intact core pieces longer than 100 mm are recovered and it becomes difficult to determine a reliable value for RMR. In these circumstances, the physical appearance of the material recovered in the core should be used as a basis for estimating GSI.

## MOHR-COULOMB PARAMETERS

Most geotechnical software is written in terms of the Mohr-Coulomb failure criterion in which the rock mass strength is defined by the cohesive strength c′ and the angle of friction ϕ′. The linear relationship between the major and minor principal stresses, $\sigma_1'$ and $\sigma_3'$, for the Mohr-Coulomb criterion is

$$\sigma_1' = \sigma_{cm} + k\sigma_3' \qquad (11)$$

where $\sigma_{cm}$ is the uniaxial compressive strength of the rock mass and k is the slope of the line relating $\sigma_1'$ and $\sigma_3'$. The values of ϕ′ and c′ can be calculated from

$$\sin\phi' = \frac{k-1}{k+1} \qquad (12)$$

$$c' = \frac{\sigma_{cm}}{2\sqrt{k}} \qquad (13)$$

There is no direct correlation between equation (11) and the non-linear Hoek-Brown criterion defined by equation (1). Consequently, determination of the values of c′ and ϕ′ for a rock mass that has been evaluated as a Hoek-Brown material is a difficult problem.

The authors believe that the most rigorous approach available, for the original Hoek-Brown criterion, is that developed by Dr J.W. Bray and reported by Hoek [17]. For any point on a surface of concern in an analysis such as a slope stability calculation, the effective normal stress is calculated using an appropriate stress analysis technique. The shear strength developed at that value of effective normal stress is then calculated from the equations given in Appendix A. The difficulty in applying this approach in practice is that most of the geotechnical software currently available provides for constant rather than effective normal stress dependent values of c′ and ϕ′.
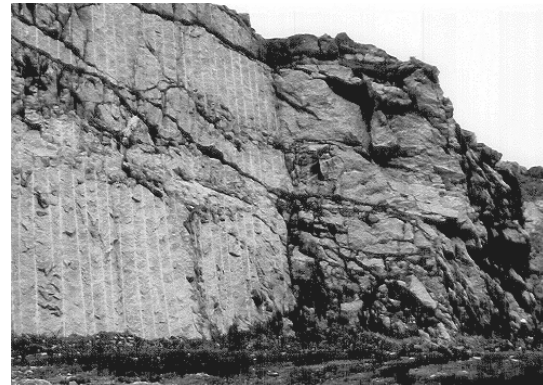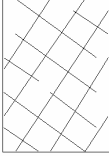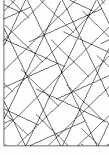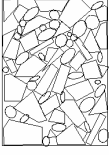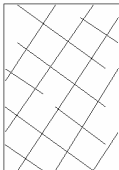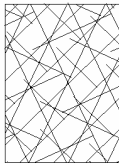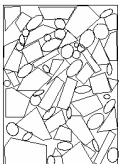


Fig. 5: Comparison between the results achieved by controlled blasting (on the left) and normal bulk blasting for a surface excavation in gneiss.

Table 4. Characterisation of rock masses on the basis of interlocking and joint alteration[1].

| ROCK MASS CHARACTERISTICS FOR STRENGTH ESTIMATES<br><br>Based upon the appearance of the rock, choose the category that you think gives the best description of the 'average' undisturbed in situ conditions. Note that exposed rock faces that have been created by blasting may give a misleading impression of the quality of the underlying rock. Some adjustment for blast damage may be necessary and examination of diamond drill core or of faces created by pre-split or smooth blasting may be helpful in making these adjustments. It is also important to recognize that the Hoek-Brown criterion should only be applied to rock masses where the size of individual blocks is small compared with the size of the excavation under consideration.<br><br>STRUCTURE | SURFACE CONDITIONS | VERY GOOD Very rough, fresh unweathered surfaces | GOOD Rough, slightly weathered, iron stained surfaces | FAIR Smooth, moderately weathered or altered surfaces | POOR Slickensided, highly weathered surfaces with compact coatings or fillings of angular fragments | VERY POOR Slickensided, highly weathered surfaces with soft clay coatings or fillings |
|---|---|---|---|---|---|---|
| | | DECREASING SURFACE QUALITY ⇨ | | | | |
| BLOCKY - very well interlocked undisturbed rock mass consisting of cubical blocks formed by three orthogonal discontinuity sets | DECREASING INTERLOCKING OF ROCK PIECES | B/VG | B/G | B/F | B/P | B/VP |
| VERY BLOCKY - interlocked, partially disturbed rock mass with multifaceted angular blocks formed by four or more discontinuity sets | | VB/VG | VB/G | VB/F | VB/P | VB/VP |
| BLOCKY/DISTURBED- folded and/or faulted with angular blocks formed by many intersecting discontinuity sets | | BD/VG | BD/G | BD/F | BD/P | BD/VP |
| DISINTEGRATED - poorly inter-locked, heavily broken rock mass with a mixture or angular and rounded rock pieces | ⇩ | D/VG | D/G | D/F | D/P | D/VP |

---

[1] In earlier versions of this table the terms BLOCKY/SEAMY and CRUSHED were used, following the terminology used by Terzaghi [9]. However, these terms proved to be misleading and they have been replaced, in this table by BLOCKY/DISTURBED, which more accurately reflects the increased mobility of a rock mass which has undergone some folding and/or faulting, and DISINTEGRATED which encompasses a wider range of particle shapes.

Table 5. Estimate of Geological Strength Index GSI based on geological descriptions.

| GEOLOGICAL STRENGTH INDEX<br><br>From the letter codes describing the structure and surface conditions of the rock mass (from Table 4), pick the appropriate box in this chart. Estimate the average value of the Geological Strength Index (GSI) from the contours.<br>Do not attempt to be too precise. Quoting a range of GSI from 36 to 42 is more realistic than stating that GSI = 38. | SURFACE CONDITIONS | VERY GOOD<br>Very rough,fresh unweathered surfaces | GOOD<br>Rough, slightly weathered, iron stained surfaces | FAIR<br>Smooth, moderately weathered or altered surfaces | POOR<br>Slickensided, highly weathered surfaces with compact coatings or fillings of angular fragments | VERY POOR<br>Slickensided, highly weathered surfaces with soft clay coatings or fillings |
|---|---|---|---|---|---|---|
| STRUCTURE | | DECREASING SURFACE QUALITY ⇨ | | | | |
| BLOCKY - very well interlocked undisturbed rock mass consisting of cubical blocks formed by three orthogonal discontinuity sets | ⇧ DECREASING INTERLOCKING OF ROCK PIECES | 80 / 70 | | | | |
| VERY BLOCKY - interlocked, partially disturbed rock mass with multifaceted angular blocks formed by four or more discontinuity sets | | | 60 / 50 | | | |
| BLOCKY/DISTURBED- folded and/or faulted with angular blocks formed by many intersecting discontinuity sets | | | | 40 / 30 | | |
| DISINTEGRATED - poorly inter-locked, heavily broken rock mass with a mixture or angular and rounded rock pieces | | | | | 20 | 10 |

Having evaluated a large number of possible approaches to this problem, it has been concluded that the most practical solution is to treat the problem as an analysis of a set of full-scale triaxial strength tests. The results of such tests are simulated by using the Hoek-Brown equation (1) to generate a series of triaxial test values. Equation (11) is then fitted to these test results by linear regression analysis and the values of c′ and ϕ′ are determined from equations (12) and (13).

A discussion of all the steps required to determine the parameters A and B (equation (2)) and c′ and ϕ′ is given in Appendix C. A spreadsheet for carrying out this analysis, with a listing of all the cell formulae, is also given in this appendix.

The values of c′ and ϕ′ obtained from this analysis are very sensitive to the range of values of the minor principal stress $\sigma_3'$ used to generate the simulated full-scale triaxial test results. On the basis of trial and error, it has been found that the most consistent results are obtained when 8 equally spaced values of $\sigma_3'$ are used in the range $0 < \sigma_3' < 0.25\,\sigma_{ci}$.

An example of the results, which are obtained from this analysis, is given in Fig. 6. Plots of the values of the ratio $c'/\sigma_{ci}$ and the friction angle ϕ′, for different combinations of GSI and $m_i$ are given in Fig. 7 and Fig. 8.

Appendix C includes a calculation for a tangent to the Mohr envelope defined by equation (2). A normal stress has to be specified in order to calculate this tangent and, in Fig. 6, this stress has been chosen so that the friction angle ϕ′ is the same for both the tangent and the line defined by c′ = 3.3 MPa and ϕ′ = 30.1°, determined by the linear regression analysis described earlier. The cohesion intercept for the tangent is c′ = 4.1 MPa which is approximately 25% higher than that obtained by linear regression analysis of the simulated triaxial test data.

Fitting a tangent to the curved Mohr envelope gives an upper bound value for the cohesive intercept c′. It is recommended that this value be reduced by about 25% in order to avoid over-estimation of the rock mass strength.

There is a particular class of problem for which extreme caution should be exercised when applying the approach outlined above. In some rock slope stability problems, the effective normal stress on some parts of the failure surface can be quite low, certainly less than 1 MPa. It will be noted that in the example given in Fig. 6, for values of $\sigma_n'$ of less than about 5 MPa, the straight line, constant c′ and ϕ′ method overestimates the available shear strength of the rock mass by increasingly significant amounts as $\sigma_n'$ approaches zero. Under such circumstances, it

would be prudent to use values of c′ and ϕ′ based on a tangent to the shear strength curve in the range of $\sigma_n'$ values applying in practice.

$$\sigma_1' = \sigma_{cm} + \frac{1+\sin\phi'}{1-\sin\phi'}\sigma_3'$$

$$\sigma_1' = \sigma_3' + \sigma_{ci}\left(m_b\frac{\sigma_3'}{\sigma_{ci}}+s\right)^a$$

$$\tau = A\sigma_{ci}\left(\frac{\sigma_n'-\sigma_{tm}}{\sigma_{ci}}\right)^B$$
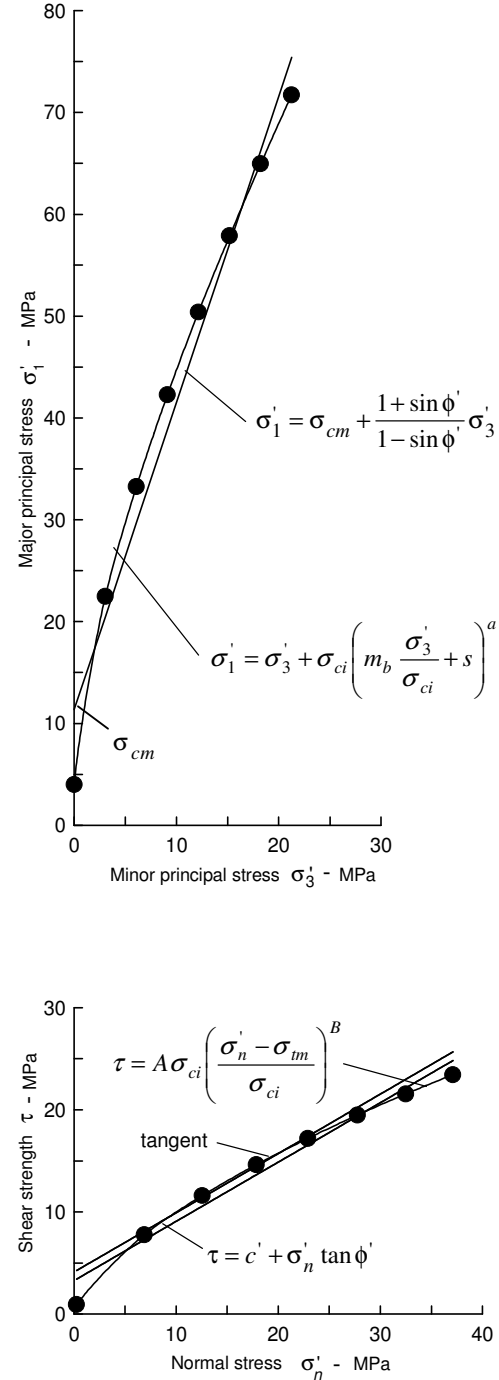
tangent

$$\tau = c' + \sigma_n'\tan\phi'$$

Fig. 6. Plot of results from simulated full scale triaxial tests on a rock mass defined by a uniaxial compressive strength $\sigma_{ci}$ = 85 MPa, a Hoek-Brown constant $m_i$ = 10 and Geological Strength Index GSI = 45. Detailed calculations are given in Appendix C.
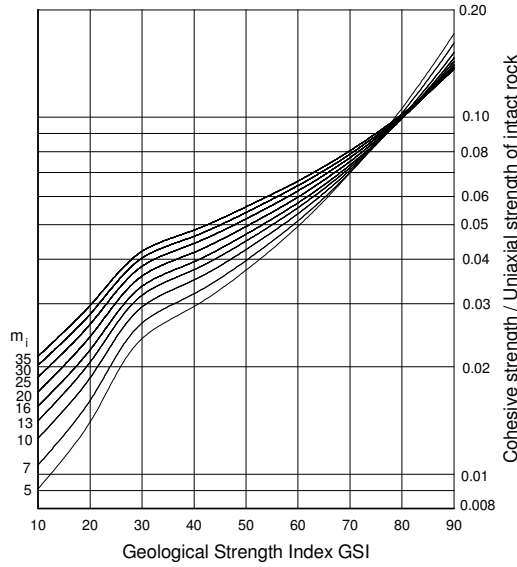
Fig. 7. Relationship between ratio of cohesive strength to uniaxial compressive strength of intact rock $c'/\sigma_{ci}$ and GSI for different $m_i$ values.
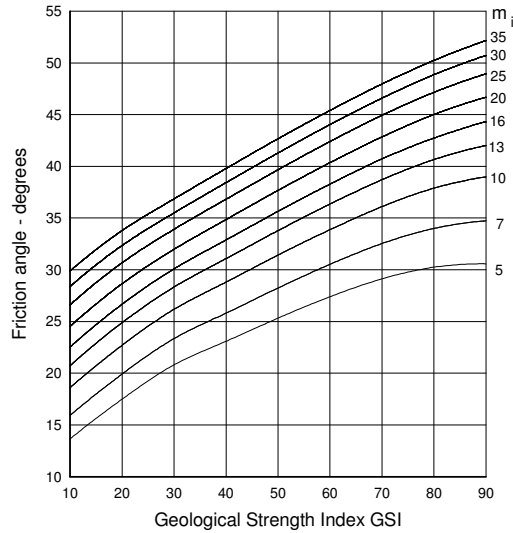


Fig. 8. Friction angle $\phi'$ for different GSI and $m_i$ values.

## DEFORMATION MODULUS

Serafim and Pereira [18] proposed a relationship between the in-situ modulus of deformation and Bieniawski's RMR classification. This relationship is based upon back analysis of dam foundation deformations and it has been found to work well for better quality rocks. However, for many of the poor quality rocks it appears to predict deformation modulus values which are too high.

Based upon practical observations and back analysis of excavation behaviour in poor quality rock masses, the following modification to Serafim and Pereira's equation is proposed for $\sigma_{ci} < 100$:

$$E_m(\text{GPa}) = \sqrt{\frac{\sigma_{ci}}{100}} 10^{\left(\frac{GSI-10}{40}\right)} \qquad (14)$$

Note that GSI has been substituted for RMR in this equation and that the modulus $E_m$ is reduced progressively as the value of $\sigma_{ci}$ falls below 100. This reduction is based upon the reasoning that the deformation of better quality rock masses is controlled by the discontinuities while, for poorer quality rock masses, the deformation of the intact rock pieces contributes to the overall deformation process.

Based upon measured deformations, equation (14) appears to work reasonably well in those cases where it has been applied. However, as more field evidence is gathered it may be necessary to modify this relationship.
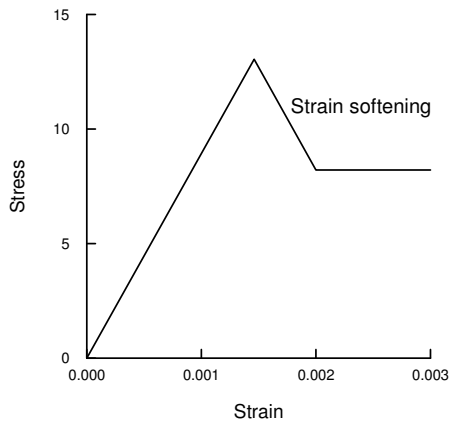
## POST-FAILURE BEHAVIOUR

When using numerical models to study the progressive failure of rock masses, estimates of the post-peak or post-failure characteristics of the rock mass are required. In some of these models, the Hoek-Brown failure criterion is treated as a yield criterion and the analysis is carried out using plasticity theory [e.g. 19]. No definite rules for dealing with this problem can be given but, based upon experience in numerical analysis of a variety of practical problems, the post-failure characteristics illustrated in Fig. 9 are suggested as a starting point.
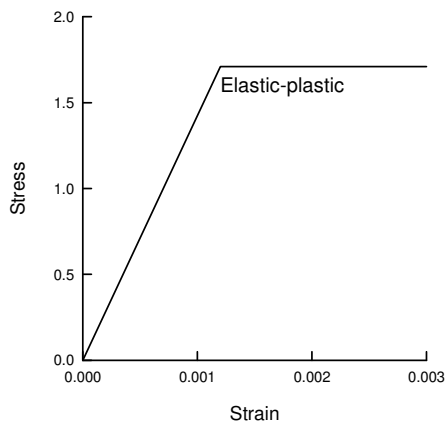
Very good quality hard rock masses

For very good quality hard rock masses, such as massive granites or quartzites, the analysis of spalling around highly stressed openings [12] suggests that the rock mass behaves in an elastic brittle manner as shown in Fig. 9(a). When the strength of the rock mass is exceeded, a sudden strength drop occurs. This is associated with significant dilation of the broken rock pieces. If this broken rock is confined, for example by rock support, then it can be assumed to behave as a rock fill with a friction angle of approximately $\phi' = 38°$ and zero cohesive strength.
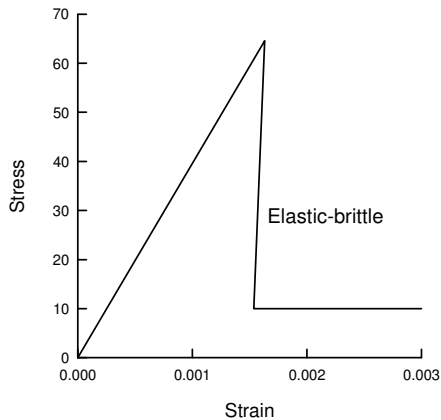
(a) Very good quality hard rock mass



(b) Average quality rock mass



(c) Very poor quality soft rock mass

Fig. 9. Suggested post-failure characteristics for different quality rock masses. Note that the stress scales are different.

Typical properties for this very good quality hard rock mass may be as follows:

| | | |
|---|---|---|
| Intact rock strength | $\sigma_{ci}$ | 150 MPa |
| Hoek-Brown constant | $m_i$ | 25 |
| Geological Strength Index | GSI | 75 |
| Friction angle | $\phi'$ | 46° |
| Cohesive strength | $c'$ | 13 MPa |
| Rock mass compressive strength | $\sigma_{cm}$ | 64.8 MPa |
| Rock mass tensile strength | $\sigma_{tm}$ | -0.9 MPa |
| Deformation modulus | $E_m$ | 42000 MPa |
| Poisson's ratio | $\nu$ | 0.2 |
| Dilation angle | $\alpha$ | $\phi'/4 = 11.5°$ |
| Post-peak characteristics | | |
| Friction angle | $\phi_f'$ | 38° |
| Cohesive strength | $c_f'$ | 0 |
| Deformation modulus | $E_{fm}$ | 10000 MPa |

Average quality rock mass

In the case of an average quality rock mass it is reasonable to assume that the post-failure characteristics can be estimated by reducing the GSI value from the in-situ value to a lower value which characterises the broken rock mass.

The reduction of the rock mass strength from the in-situ to the broken state corresponds to the strain softening behaviour illustrated in Fig. 9(b). In this figure it has been assumed that post failure deformation occurs at a constant stress level, defined by the compressive strength of the broken rock mass. The validity of this assumption is unknown.

Typical properties for this average quality rock mass may be as follows:

| | | |
|---|---|---|
| Intact rock strength | $\sigma_{ci}$ | 80 MPa |
| Hoek-Brown constant | $m_i$ | 12 |
| Geological Strength Index | GSI | 50 |
| Friction angle | $\phi'$ | 33° |
| Cohesive strength | $c'$ | 3.5 MPa |
| Rock mass compressive strength | $\sigma_{cm}$ | 13 MPa |
| Rock mass tensile strength | $\sigma_{tm}$ | -0.15 |
| Deformation modulus | $E_m$ | 9000 MPa |
| Poisson's ratio | $\nu$ | 0.25 |
| Dilation angle | $\alpha$ | $\phi'/8 = 4°$ |
| Post-peak characteristics | | |
| Broken rock mass strength | $\sigma_{fcm}$ | 8 MPa |
| Deformation modulus | $E_{fm}$ | 5000 MPa |

Very poor quality rock mass

Analysis of the progressive failure of very poor quality rock masses surrounding tunnels suggests that the post-failure characteristics of the rock are adequately represented by assuming that it behaves perfectly plastically. This means that it continues to deform at a constant stress level and that no volume change is associated with this ongoing failure. This type of behaviour is illustrated in Fig. 9(c).

Typical properties for this very poor quality rock mass may be as follows:

| | | |
|---|---|---|
| Intact rock strength | $\sigma_{ci}$ | 20 MPa |
| Hoek-Brown constant | $m_i$ | 8 |
| Geological Strength Index | GSI | 30 |
| Friction angle | $\phi'$ | 24° |
| Cohesive strength | $c'$ | 0.55 MPa |
| Rock mass compressive strength | $\sigma_{cm}$ | 1.7 MPa |
| Rock mass tensile strength | $\sigma_{tm}$ | -0.01 MPa |
| Deformation modulus | $E_m$ | 1400 MPa |
| Poisson's ratio | $\nu$ | 0.3 |
| Dilation angle | $\alpha$ | zero |
| Post-peak characteristics | | |
| Broken rock mass strength | $\sigma_{fcm}$ | 1.7 MPa |
| Deformation modulus | $E_{fm}$ | 1400 MPa |

### PRACTICAL EXAMPLES

Massive weak rock masses

Karzulovic and Diaz [20] have described the results of a program of triaxial tests on a cemented breccia known as Braden Breccia from the El Teniente mine in Chile. In order to design underground openings in this rock, attempts were made to classify the rock mass in accordance with Bieniawski's RMR system. However, as illustrated in Fig. 10, this rock mass has very few discontinuities and so assigning realistic numbers to terms depending upon joint spacing and condition proved to be very difficult. Finally, it was decided to treat the rock mass as a weak but homogeneous 'almost intact' rock and to determine its properties by means of triaxial tests on large diameter specimens.

A series of triaxial tests was carried out on 100 mm diameter core samples, illustrated in Fig. 11. The results of these tests were analysed by means of the regression analysis presented in Appendix A. Back analysis of the behaviour of underground openings in this rock indicate that the in-situ GSI value is approximately 75. From the spreadsheet presented in Appendix C the following parameters were obtained:

| | | |
|---|---|---|
| Intact rock strength | $\sigma_{ci}$ | 51 MPa |
| Hoek-Brown constant | $m_i$ | 16.3 |
| Geological Strength Index | GSI | 75 |
| Hoek-Brown constant | s | 0.062 |
| Friction angle | $\phi'$ | 42° |
| Cohesive strength | $c'$ | 4.32 MPa |
| Deformation modulus | $E_m$ | 30000 MPa |



Fig. 10. Braden Breccia at El Teniente Mine in Chile. This rock is a cemented breccia with practically no joints. It was dealt with in a manner similar to weak concrete and tests were carried out on 100 mm diameter specimens illustrated in Fig. 11.



Fig. 11. 100 mm diameter by 200 mm long specimens of Braden Breccia from the El Teniente mine in Chile.

A similar approach has been used for dealing with rock masses with very sparse jointing. In one case, 50 mm diameter core specimens of a massive siltstone were successfully prepared and tested in a laboratory very close to the site in order to minimise the effects of very rapid deterioration when this material was subjected to changing moisture content conditions.

Massive strong rock masses

The Rio Grande Pumped Storage Project in Argentina includes a large underground powerhouse and surge control complex and a 6 km long tailrace tunnel. The rock mass surrounding these excavations is a massive gneiss with very few joints. A typical core from this rock mass is illustrated in Fig. 12. The appearance of the rock at the surface is illustrated in Fig. 5, which shows a cutting for the dam spillway.

| | | |
|---|---|---|
| Intact rock strength | $\sigma_{ci}$ | 110 MPa |
| Hoek-Brown constant | $m_i$ | 17.7 |
| Geological Strength Index | GSI | 75 (assumed) |
| Hoek-Brown constant | $m_b$ | 7.25 |
| Hoek-Brown constant | s | 0.062 |
| Constant | a | 0.5 |
| Friction angle | $\phi'$ | 43° |
| Cohesive strength | c′ | 9.4 MPa |
| Rock mass compressive strength | $\sigma_{cm}$ | 43 MPa |
| Rock mass tensile strength | $\sigma_{tm}$ | -0.94 MPa |
| Deformation modulus | $E_m$ | 42000 MPa |

Fig. 13 illustrates the 8 m high 12 m span top heading for the tailrace tunnel. The final tunnel height of 18 m was achieved by blasting two 5 m benches. The top heading was excavated by full-face drill and blast and, because of the excellent quality of the rock mass and the tight control on blasting quality, most of the top heading did not require any support.
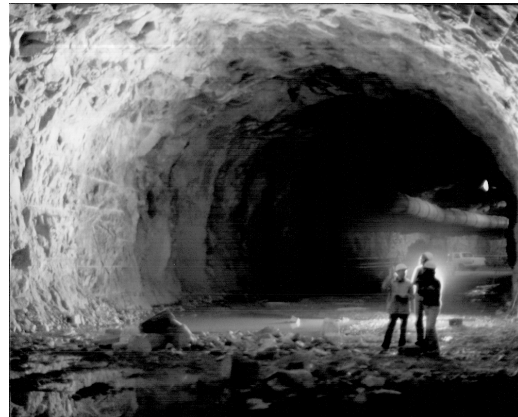


Fig. 13. Top heading for the 12 m span, 18 m high tailrace tunnel for the Rio Grande Pumped Storage Project.

Details of this project are to be found in Moretto et al [21]. Hammett and Hoek [22] have described the design of the support system for the 25 m span underground powerhouse in which a few structurally controlled wedges were identified and stabilised during excavation.

Average quality rock mass

The partially excavated powerhouse cavern in the Nathpa Jhakri Hydroelectric project in Himachel Pradesh, India is illustrated in Fig. 14. The rock is a jointed quartz mica schist, which has been extensively evaluated by the Geological Survey of India as described by Jalote et al [23]. An average GSI value of 65 was chosen to estimate the rock mass properties which were used for the cavern support design. Additional support, installed on the instructions of the Engineers, was placed in weaker rock zones.
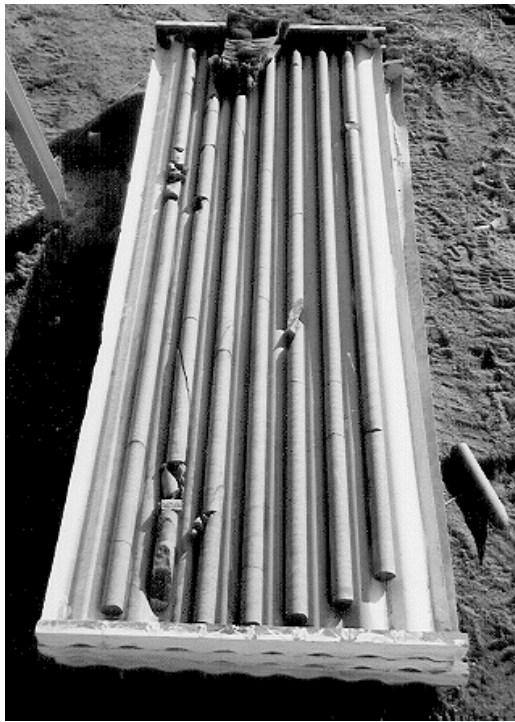


Fig. 12. Excellent quality core from a hard strong rock mass with very few discontinuities.

The rock mass can be described as BLOCKY/VERY GOOD and the GSI value, from Table 5, is 75. Typical characteristics for the rock mass are as follows:

Fig. 14. Partially completed 20 m span, 42.5 m high underground powerhouse cavern of the Nathpa Jhakri Hydroelectric project in Himachel Pradesh in India. The cavern is approximately 300 m below the surface.

The assumed rock mass properties are as follows:

| Intact rock strength | $\sigma_{ci}$ | 30 MPa |
|---|---|---|
| Hoek-Brown constant | $m_i$ | 15.6 |
| Geological Strength Index | GSI | 65 (average) |
| Hoek-Brown constant | $m_b$ | 4.5 |
| Hoek-Brown constant | s | 0.02 |
| Constant | a | 0.5 |
| Friction angle | $\phi'$ | 40° |
| Cohesive strength | $c'$ | 2.0 MPa |
| Rock mass compressive strength | $\sigma_{cm}$ | 8.2 MPa |
| Rock mass tensile strength | $\sigma_{tm}$ | -0.14 MPa |
| Deformation modulus | $E_m$ | 13000 MPa |

Two and three dimensional stress analyses of the nine stages used to excavate the cavern were carried out to determine the extent of potential rock mass failure and to provide guidance in the design of the support system. An isometric view of one of the three dimensional models is given in Figure 15.
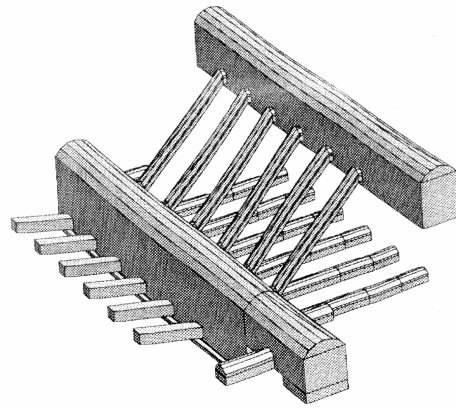


Fig. 15. Isometric view of a 3DEC[2] model of the Underground powerhouse cavern and the transformer gallery of the Nathpa Jhakri Hydroelectric project, analysed by Dr B. Dasgupta[3] .

The support for the powerhouse cavern consists of rockbolts and mesh reinforced shotcrete. Alternating 6 and 8 m long 32 mm diameter bolts on 1 x 1 m and 1.5 x 1.5 m centres are used in the arch. Alternating 9 and 7.5 m long 32 mm diameter bolts are used in the upper and lower sidewalls with alternating 9 and 11 m long 32 mm rockbolts in the centre of the sidewalls, all at a grid spacing of 1.5 m. Shotcrete consists of two 50 mm thick layers of plain shotcrete with an interbedded layer of weldmesh. The support provided by the shotcrete was not included in the support design analysis, which relies upon the rockbolts to provide all the support required.

In the headrace tunnel, some zones of sheared quartz mica schist have been encountered and these have resulted in large displacements as illustrated in Fig. 16. This is a common problem in hard rock tunnelling where the excavation sequence and support system have been designed for 'average' rock mass conditions. Unless very rapid changes in the length of blast rounds and the installed support are made when an abrupt change to poor rock conditions occurs, for example when a fault is encountered, problems with controlling tunnel deformation can arise.

---

[2] Available from ITASCA Consulting Group Inc., Thresher Square East, 708 South Third Street, Suite 310, Minneapolis, Minnesota 55415, USA. Fax 1 612 371 4717
[3] Formerly at the Institute of Rock Mechanics (Kolar), Kolar Gold Fields, Karnataka, now with of Advanced Technology and Engineering Services, Delhi. India.
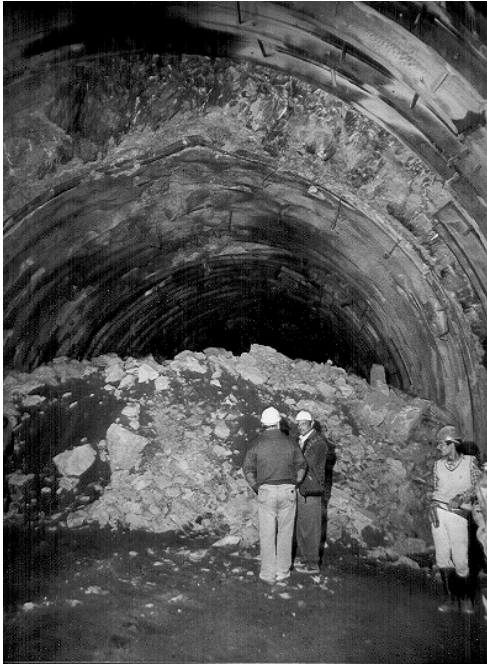
Fig. 16. Large displacements in the top heading of the headrace tunnel of the Nathpa Jhakri hydroelectric project in India.

The only effective way known to the authors for anticipating this type of problem is to keep a probe hole ahead of the advancing face at all times. Typically, a long probe hole is percussion drilled during a maintenance shift and the penetration rate, return water flow and chippings are constantly monitored during drilling. Where significant problems are indicated by this percussion drilling, one or two diamond-drilled holes may be required to investigate these problems in more detail. In some special cases, the use of a pilot tunnel may be more effective in that it permits the ground properties to be defined more accurately than is possible with probe hole drilling. In addition, pilot tunnels allow pre-drainage and pre-reinforcement of the rock ahead of the development of the full excavation profile.

Poor quality rock mass at shallow depth

Kavvadas et al [24] have described some of the geotechnical issues associated with the construction of 18 km of tunnels and the 21 underground stations of the Athens Metro. These excavations are all shallow with typical depths to tunnel crown of between 15 and 20 m. The principal problem is one of surface subsidence rather than failure of the rock mass surrounding the openings.
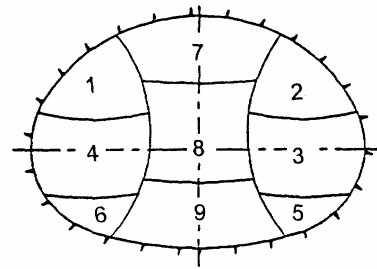


Fig. 17. Twin side drift and central pillar excavation method. Temporary support consists of double wire mesh reinforced 250 - 300 mm thick shotcrete shells with embedded lattice girders or HEB 160 steel sets at 0.75 - 1 m spacing.
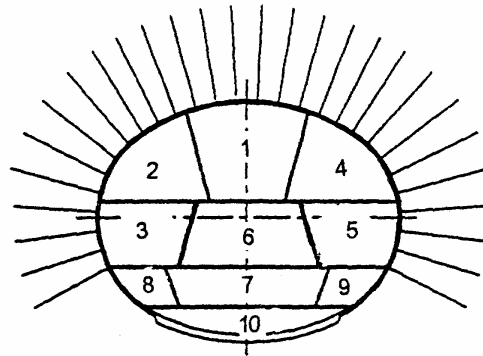


Fig. 18. Top heading and bench method of excavation. Temporary support consists of a 200 mm thick shotcrete shell with 4 and 6 m long untensioned grouted rockbolts at 1.0 - 1.5 m spacing.
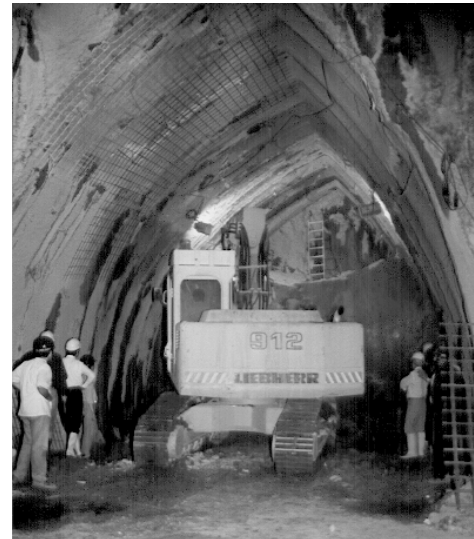


Fig. 19. Side drift in the Athens Metro Olympion station excavation, which was excavated by the method illustrated in Fig. 17. The station has cover depth of approximately 10 m over the crown.

The rock mass is locally known as Athenian schist which is a term erroneously used to describe a

sequence of Upper Cretaceous flysch-type sediments including thinly bedded clayey and calcareous sandstones, siltstones (greywackes), slates, shales and limestones. During the Eocene, the Athenian schist formations were subjected to intense folding and thrusting. Later extensive faulting caused extensional fracturing and widespread weathering and alteration of the deposits.

The GSI values, estimated from Bieniawski's 1976 RMR classification, modified as recommended by Hoek, Kaiser and Bawden [12], ranges from about 15 to about 45. The higher values correspond to the intercalated layers of sandstones and limestones, which can be described as BLOCKY/DISTURBED and POOR (Table 5). The completely decomposed schist can be described as DISINTEGRATED and VERY POOR and has GSI values ranging from 15 to 20. Rock mass properties for the completely decomposed schist, using a GSI value of 20, are as follows:

| | | |
|---|---|---|
| Intact rock strength | $\sigma_{ci}$ | 5-10 MPa |
| Hoek-Brown constant | $m_i$ | 9.6 |
| Geological Strength Index | GSI | 20 |
| Hoek-Brown constant | $m_b$ | 0.55 |
| Hoek-Brown constant | s | 0 |
| Constant | a | 0.55 |
| Friction angle | $\phi'$ | 22.4° |
| Cohesive strength | $c'$ | 0.09-0.18 MPa |
| Rock mass strength | $\sigma_{cm}$ | 0.27-0.53 MPa |
| Deformation modulus | $E_m$ | 398-562 MPa |

The Academia, Syntagma, Omonia and Olympion stations were constructed using the New Austrian Tunnelling Method twin side drift and central pillar method as illustrated in Fig. 17. The more conventional top heading and bench method, illustrated in Fig. 18, was used for the excavation of the Ambelokipi station. These stations are all 16.5 m wide and 12.7 m high. The appearance of the rock mass in one of the Olympion station side drift excavations is illustrated in Fig. 19 and Fig. 20.

Numerical analyses of the two excavation methods illustrated in Fig. 17 and Fig. 18 showed that the twin side drift method resulted in slightly less rock mass failure in the crown of the excavation. However, the final surface displacements induced by the two excavation methods were practically identical.

Maximum vertical displacements of the surface above the centre-line of the Omonia station amounted to 51 mm. Of this, 28 mm occurred during the excavation of the side drifts, 14 mm during the removal of the central pillar and a further 9 mm occurred as a time dependent settlement after completion of the excavation. According to Kavvadas et al [24], this time dependent settlement is due to the dissipation of excess pore water pressures which were built up during excavation. In the case of the Omonia station, the excavation of recesses towards the eastern end of the station, after completion of the station excavation, added a further 10 to 12 mm of vertical surface displacement at this end of the station.



Fig.20. Appearance of the very poor quality Athenian schist at the face of the side heading illustrated in Fig. 19.

Poor quality rock mass under high stress

The Yacambú Quibor tunnel in Venezuela is considered to be one of the most difficult tunnels in the world. This 26 km long water supply tunnel through the Andes is being excavated in sandstones and phyllites at depths of up to 1200 m below surface. The graphitic phyllite is a very poor quality rock and gives rise to serious squeezing problems which, without adequate support, result in complete closure of the tunnel. A full-face tunnel-boring machine was completely destroyed in 1979 when trapped by squeezing ground conditions.

At its worst, the graphitic phyllite has an unconfined compressive strength of about 15 MPa (see Fig. 1), and the estimated GSI value is about 24. Typical rock mass properties are as follows:

| | | |
|---|---|---|
| Intact rock strength | $\sigma_{ci}$ | 15 MPa |
| Hoek-Brown constant | $m_i$ | 10 |
| Geological Strength Index | GSI | 24 |
| Hoek-Brown constant | $m_b$ | 0.66 |
| Hoek-Brown constant | s | 0 |
| Constant | a | 0.53 |
| Friction angle | $\phi'$ | 24° |
| Cohesive strength | $c'$ | 0.34 MPa |
| Rock mass strength | $\sigma_{cm}$ | 1 MPa |
| Deformation modulus | $E_m$ | 870 MPa |

Various support methods have been used on this tunnel and only one will be considered here. This was a trial section of tunnel, at a depth of about 600 m, constructed in 1989. The support of the 5.5 m span tunnel was by means of a complete ring of 5 m long, 32 mm diameter untensioned grouted dowels with a

200 mm thick shell of reinforced shotcrete. This support system proved to be very effective but was later abandoned in favour of yielding steel sets (steel sets with sliding joints) because of construction schedule considerations.
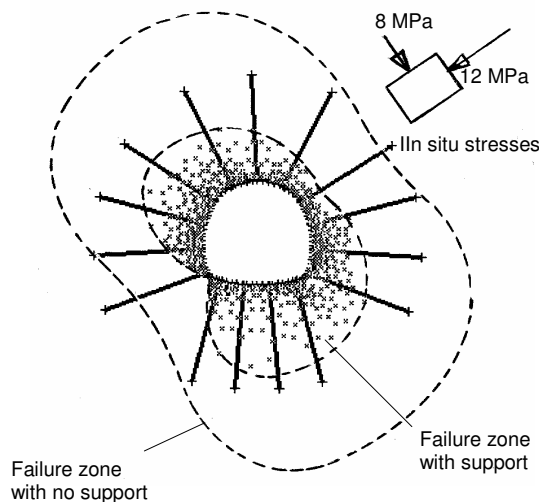


Fig. 21. Results of a numerical analysis of the failure of the rock mass surrounding the Yacambu-Quibor tunnel when excavated in graphitic phyllite at a depth of about 600 m below surface.
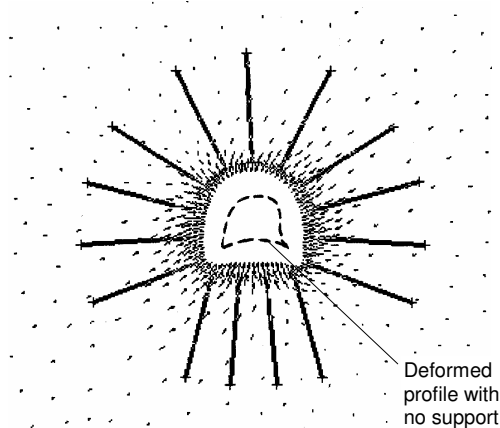


Fig. 22. Displacements in the rock mass surrounding the Yacambu-Quibor tunnel. The maximum calculated displacement is 258 mm with no support and 106 mm with support.

Examples of the results of a typical numerical stress analysis of this trial section, carried out using the program PHASE2[4], are given in Fig. 21 and Fig. 22. Fig. 21 shows the extent of failure, with and without support, while Fig. 22 shows the displacements in the rock mass surrounding the tunnel. Note that the criteria used to judge the effectiveness of the support design are that the zone of failure surrounding the tunnel should lie within the envelope of the rockbolt support, the rockbolts should not be stressed to failure and the displacements should be of reasonable magnitude and should be uniformly distributed around the tunnel. All of these objectives were achieved by the support system described earlier.

Slope stability considerations

When dealing with slope stability problems in rock masses, great care has to be taken in attempting to apply the Hoek-Brown failure criterion, particularly for small steep slopes. As illustrated in Fig. 23, even rock masses which appear to be good candidates for the application of the criterion can suffer shallow structurally controlled failures under the very low stress conditions which exist in such slopes.

As a general rule, when designing slopes in rock, the initial approach should always be to search for potential failures controlled by adverse structural conditions. These may take the form of planar failures on outward dipping features, wedge failures on intersecting features, toppling failures on inward dipping failures or complex failure modes involving all of these processes. Only when the potential for structurally controlled failures has been eliminated should consideration be given to treating the rock mass as an isotropic material as required by the Hoek-Brown failure criterion (see Fig. 4).

Fig. 24 illustrates a case in which the base of a slope failure is defined by an outward dipping fault which does not daylight at the toe of the slope. Circular failure through the poor quality rock mass overlying the fault allows failure of the toe of the slope. Analysis of this problem was carried out by assigning the rock mass at the toe properties which had been determined by application of the Hoek-Brown criterion. A search for the critical failure surface was carried out utilising the program XSTABL[5] which allows complex failure surfaces to be analysed and which includes facilities for the input of non-linear failure characteristics as defined by equation 2.
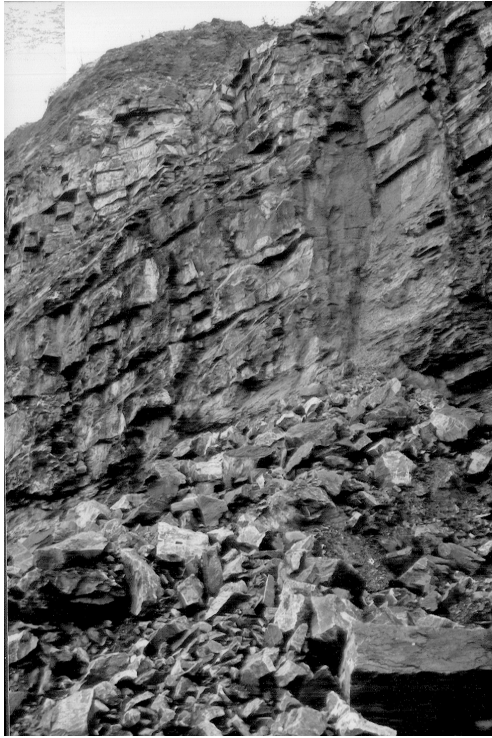
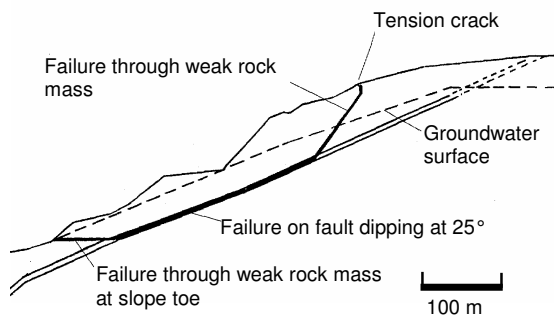Fig. 23. Structurally controlled failure in the face of a steep bench in a heavily jointed rock mass.



Fig 24. Complex slope failure controlled by an outward dipping basal fault and circular failure through the poor quality rock mass overlying the toe of the slope.

Sancio [25] and Sönmez et al [26] have presented interesting discussions on methods of back analysis of slope failures involving jointed rock masses, the properties of which can be described in terms of the Hoek-Brown failure criterion. Numerical analysis of complex failure processes in very large-scale open pit mine slopes have been described by Board et al [27].

## REFERENCES

1. Hoek E. and Brown E.T. Underground excavations in rock, p. 527. London, Instn Min. Metall. (1980).
2. Broch E. The influence of water on some rock properties. Proc. 3$^{rd}$ Congress, ISRM, Denver. 74(2), Part A, 33-38 (1974).
3. Terzaghi K. Die Berechnung der Durchlassigkeitsziffer des Tones aus dem Verlauf der hydrodynamischen Spannungserscheinungen. Sber. Akad. Wiss. Wien. 132(105), 125-138 (1923).
4. Lade P.V. and de Boer R. The concept of effective stress for soil, concrete and rock. Géotechnique 47(1), 61-78 (1997).
5. Brace W.F. and Martin R.J. A test of the law of effective stress for crystalline rocks of low porosity. Int. J. Rock Mech. Min. Sci.. 5(5), 415-426 (1968).
6. Brown E.T. (Ed). Rock characterization, testing and monitoring - ISRM suggested methods, 171-183. Oxford, Pergamon (1981).
7. Martin C.D. and Chandler N.A. The progressive failure of Lac du Bonnet granite. Int. J. Rock Mech. Min. Sci. & Geomech. Abstr. 30(7), 643-659 (1994).
8. Salcedo D.A. Macizos Rocosos: Caracterización, Resistencia al Corte y Mecanismos de Rotura. Proc. 25 Aniversario Conferencia Soc. Venezolana de Mecánica del Suelo e Ingeniería de Fundaciones, Caracas. 143-172 (1983).
9. Medhurst T.P., Brown E.T. and Trueman R. Experimental studies of the effects of scale on the strength of coal. In Proc. 8th Int. Congr. Rock Mech, 1, 347-351. Rotterdam, Balkema (1995).

10. Medhurst T.P. and Brown E.T. Large scale laboratory testing of coal. In Proc. 7th ANZ Conf. Geomech., (Edited by Jaksa M.B., Kaggwa W.S. and Cameron D.A.), 203-208, Canberra, IE Australia (1996).

11. Hoek E. Strength of rock and rock masses, ISRM News Journal, 2(2), 4-16 (1994).

12. Hoek E., Kaiser P.K. and Bawden W.F. Support of underground excavations in hard rock. p. 215. Rotterdam, Balkema. (1995).

13. Terzaghi K. Rock defects and loads on tunnel supports. In Rock tunneling with steel supports, (Edited by Proctor R. V. and White T. L.) 1, 17-99. Youngstown, Ohio, Commercial Shearing and Stamping Company (1946).

14. Hoek E., Wood D. and Shah S. A modified Hoek-Brown criterion for jointed rock masses. Proc. Rock Characterization, Symp. Int. Soc. Rock Mech.: Eurock '92, (Edited by Hudson J.A.), 209-214. London, Brit. Geotech. Soc. (1992).

15. Bieniawski Z.T. Rock mass classification in rock engineering. In Exploration for Rock Engineering, Proc. of the Symp., (Edited by Bieniawski Z.T.) 1, 97-106. Cape Town, Balkema (1976).

16. Bieniawski Z.T. Engineering Rock Mass Classifications. p. 251. New York, Wiley (1989).

17. Hoek E. Strength of jointed rock masses, 1983 Rankine Lecture. Géotechnique 33(3), 187-223. (1983).

18. Serafim J.L. and Pereira J.P. Consideration of the geomechanical classification of Bieniawski. Proc. Int. Symp. on Engineering Geology and Underground Construction, Lisbon 1(II), 33-44. (1983).

19. Pan X.D. and Hudson J.A. A simplified three dimensional Hoek-Brown yield criterion. In Rock Mechanics and Power Plants, Proc. ISRM Symp. (Edited by Romana M.), 95-103. Rotterdam, Balkema (1988).

20. Karzulovic A. and Díaz, A. Evaluación de las Propiedades Geomacánicas de la Brecha Braden en Mina El Teniente. Proc. IV Congreso Sudamericano de Mecanica de Rocas, Santiago 1, 39-47. (1994).

21. Moretto O., Sarra Pistone R.E. and Del Rio J.C. A case history in Argentina - Rock Mechanics for underground works in the Pumping Storage Development of Rio Grande No 1. In Comprehensive Rock Engineering. (Edited by Hudson. J.A.) 5, 159-192. Oxford, Pergamon (1993).

22. Hammett R.D. and Hoek E. Design of large underground caverns for hydroelectric projects with particular reference to structurally controlled failure mechanisms. In Recent Developments in Geotechnical Engineering for Hydro Projects. (Edited by Kulhawy F.H.), 192-206. New York, ASCE (1981).

23. Jalote P.M., Kumar A. and Kumar V. Geotechniques applied in the design of the machine hall cavern, Nathpa Jhakri Hydel Project, N.W. Himalaya, India. J. Engng Geol. (India) XXV(1-4), 181-192. (1996).

24. Kavvadas M., Hewison L.R., Lastaratos P.G., Seferoglou C. and Michalis I. Experience in the construction of the Athens Metro. Proc. Int. Symp. Geotechical Aspects of Underground Construction in Soft Ground. (Edited by Mair R.J. and Taylor R.N.), 277-282. London, City University. (1996).

25. Sancio R.T. The use of back-calculations to obtain shear and tensile strength of weathered rock. Proc. Int. Symp. Weak Rock, Tokyo 2, 647-652. (1981).

26. Sönmez H., Ulusay R. and Gökçeoglu, C. Practical procedure for the back analysis of slope failures in closely jointed rock masses. Submitted to Int. J. Rock Mech. Min. Sci. (1997).

27. Board M., Chacon E., Verona P. and Lorig L. Comparative analysis of toppling behaviour at Chuquicamata open pit mine, Chile. Trans. Instn Min. Metall.. 105, A11-21. (1996).

28. Balmer G. A general analytical solution for Mohr's envelope. Am. Soc. Test. Mat. 52, 1260-1271. (1952).

29. Hoek E. and Brown E.T. The Hoek-Brown failure criterion - a 1988 update. In Rock Engineering for Underground Excavations, Proc. 15th Canadian Rock Mech. Symp. (Edited by Curran J.C.), 31-38. Toronto, Dept. Civil Engineering, University of Toronto. (1988).

30. Hoek E. and Franklin J.A. A simple triaxial cell for field and laboratory testing of rock. Trans. Instn Min. Metall. 77, A22-26.

## APPENDIX A - HISTORICAL DEVELOPMENT OF THE HOEK-BROWN CRITERION

| Publication | Coverage | Equations |
|---|---|---|
| Hoek & Brown [1] | Original criterion for heavily jointed rock masses with no fines. Mohr envelope was obtained by statistical curve fitting to a number of $(\sigma'_n, \tau)$ pairs calculated by the method published by Balmer [28]. $\sigma'_1, \sigma'_3$ are major and minor effective principal stresses at failure, respectively $\sigma_t$ is the tensile strength of the rock mass $m$ and $s$ are material constants $\sigma'_n, \tau$ are effective normal and shear stresses, respectively. | $\sigma'_1 = \sigma'_3 + \sigma_{ci}\sqrt{m\sigma'_3/\sigma_{ci} + s}$ $\sigma_t = \frac{\sigma_{ci}}{2}\left(m - \sqrt{m^2 + 4s}\right)$ $\tau = A\sigma_{ci}\left((\sigma'_n - \sigma_t)/\sigma_{ci}\right)^B$ $\sigma'_n = \sigma'_3 + \left((\sigma'_1 - \sigma'_3)/(1 + \partial\sigma'_1/\partial\sigma'_3)\right)$ $\tau = (\sigma'_n - \sigma'_3)\sqrt{\partial\sigma'_1/\partial\sigma'_3}$ $\partial\sigma'_1/\partial\sigma'_3 = m\sigma_{ci}/2(\sigma'_1 - \sigma'_3)$ |
| Hoek [17] | Original criterion for heavily jointed rock masses with no fines with a discussion on anisotropic failure and an exact solution for the Mohr envelope by Dr J.W. Bray. | $\sigma'_1 = \sigma'_3 + \sigma_{ci}\sqrt{m\sigma'_3/\sigma_{ci} + s}$ $\tau = \left(Cot\phi'_i - Cos\phi'_i\right)m\sigma_{ci}/8$ $\phi'_i = \arctan\left(1/\sqrt{4h\cos^2\theta - 1}\right)$ $\theta = \left(90 + \arctan(1/\sqrt{h^3 - 1})\right)/3$ $h = 1 + \left(16(m\sigma'_n + s\sigma_{ci})/(3m^2\sigma_{ci})\right)$ |
| Hoek & Brown [29] | As for Hoek [17] but with the addition of relationships between constants $m$ and $s$ and a modified form of *RMR* (Bieniawski [15]) in which the Groundwater rating was assigned a fixed value of 10 and the Adjustment for Joint Orientation was set at 0. Also a distinction between *disturbed* and *undisturbed* rock masses was introduced together with means of estimating deformation modulus $E$ (after Serafim and Pereira [18]). | *Disturbed rock masses:* $m_b/m_i = \exp((RMR - 100)/14)$ $s = \exp((RMR - 100)/6)$ *Undisturbed or interlocking rock masses* $m_b/m_i = \exp((RMR - 100)/28)$ $s = \exp((RMR - 100)/9)$ $E = 10^{((RMR - 10)/40)}$ $m_b, m_i$ are for broken and intact rock, respectively. |
| Hoek, Wood & Shah [14] | Modified criterion to account for the fact the heavily jointed rock masses have zero tensile strength. Balmer's technique for calculating shear and normal stress pairs was utilised | $\sigma'_1 = \sigma'_3 + \sigma_{ci}\left(m_b\sigma'_3/\sigma_{ci}\right)^\alpha$ $\sigma'_n = \sigma'_3 + \left((\sigma'_1 - \sigma'_3)/(1 + \partial\sigma'_1/\partial\sigma'_3)\right)$ $\tau = (\sigma'_n - \sigma'_3)\sqrt{\partial\sigma'_1/\partial\sigma'_3}$ $\partial\sigma'_1/\partial\sigma'_3 = 1 + \alpha m_b^\alpha\left(\sigma'_3/\sigma_{ci}\right)^{(\alpha - 1)}$ |
| Hoek [11] Hoek, Kaiser & Bawden [12] | Introduction of the Generalised Hoek-Brown criterion, incorporating both the original criterion for fair to very poor quality rock masses and the modified criterion for very poor quality rock masses with increasing fines content. The Geological Strength Index *GSI* was introduced to overcome the deficiencies in Bieniawski's *RMR* for very poor quality rock masses. The distinction between disturbed and undisturbed rock masses was dropped on the basis that disturbance is generally induced by engineering activities and should be allowed for by downgrading the value of *GSI*. | $\sigma'_1 = \sigma'_3 + \sigma_c\left(m\sigma'_3/\sigma_{ci} + s\right)^a$ for *GSI* >25 $m_b/m_i = \exp((GSI - 100)/28)$ $s = \exp((GSI - 100)/9)$ $a = 0.5$ for *GSI* < 25 $s = 0$ $a = 0.65 - GSI/200$ |

## APPENDIX B - TRIAXIAL TESTS TO DETERMINE $\sigma_{ci}$ AND $m_i$

Determination of the intact rock uniaxial compressive strength $\sigma_{ci}$ and the Hoek-Brown constant $m_i$ should be carried out by triaxial testing wherever possible. The tests should be carried out over a confining stress range from zero to one half of the uniaxial compressive strength. At lease five data points should be included in the analysis.

One type of triaxial cell which can be used for these tests is illustrated in Fig. B1. This cell, described by Hoek and Franklin [26], does not require draining between tests and is convenient for the rapid testing or a large number of specimens. More sophisticated cells are available for research purposes but the results obtained from the cell illustrated in Fig. B1 are adequate for the rock strength estimates described in this paper. This cell has the additional advantage that it can be used in the field when testing materials such as coals, shales and phyllites which are extremely difficult to preserve during transportation and normal specimen preparation for laboratory testing.

Once the five or more triaxial test results have been obtained, they can be analysed to determine the uniaxial compressive strength $\sigma_{ci}$ and the Hoek-Brown constant $m_i$ as described by Hoek and Brown [1]. In this analysis, equation (4) is re-written in the form:

$$y = m\sigma_{ci}x + s\sigma_{ci} \tag{B1}$$

where $x = \sigma_3'$ and $y = (\sigma_1' - \sigma_3')^2$

The uniaxial compressive strength $\sigma_{ci}$ and the constant $m_i$ are calculated from:

$$\sigma_{ci}^2 = \frac{\sum y}{n} - \left[ \frac{\sum xy - \left( \sum x \sum y / n \right)}{\sum x^2 - \left( \left( \sum x \right)^2 / n \right)} \right] \frac{\sum x}{n} \tag{B2}$$

$$m_i = \frac{1}{\sigma_{ci}} \left[ \frac{\sum xy - \left( \sum x \sum y / n \right)}{\sum x^2 - \left( \left( \sum x \right)^2 / n \right)} \right] \tag{B3}$$

The coefficient of determination $r^2$ is given by:

$$r^2 = \frac{\left[ \sum xy - \left( \sum x \sum y / n \right) \right]^2}{\left[ \sum x^2 - \left( \sum x \right)^2 / n \right] \left[ \sum y^2 - \left( \sum y \right)^2 / n \right]} \tag{B4}$$
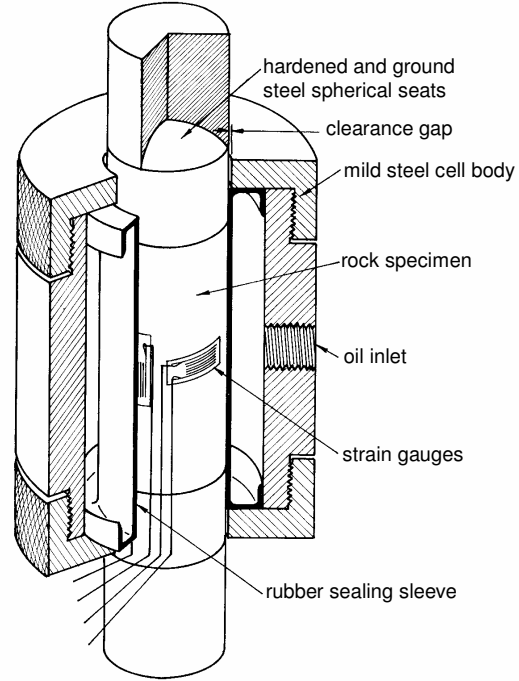


Fig. B1. Cut-away view of the triaxial cell designed by Hoek and Franklin [26].

Fig. B2. Spreadsheet for calculation of $\sigma_{ci}$ and $m_i$ from triaxial test data

| Triaxial test data | | | | | | Calculation | | |
|---|---|---|---|---|---|---|---|---|
| x | | y | xy | xsq | ysq | Number of tests | n = | 5 |
| sig3 | sig1 | | | | | Uniaxial strength | sigci = | 37.4 |
| 0 | 38.3 | 1466.89 | 0.0 | 0.0 | 2151766 | Hoek-Brown constant | mi = | 15.50 |
| 5 | 72.4 | 4542.76 | 22713.8 | 25.0 | 20636668 | Hoek-Brown constant | s = | 1.00 |
| 7.5 | 80.5 | 5329.00 | 39967.5 | 56.3 | 28398241 | Coefficient of determination r2 = | | 0.997 |
| 15 | 115.6 | 10120.36 | 151805.4 | 225.0 | 102421687 | | | |
| 20 | 134.3 | 13064.49 | 261289.8 | 400.0 | 170680899 | | | |
| | | | | | | | | |
| 47.5 | 441.1 | 34523.50 | 475776.5 | 706.3 | 324289261 | | | |
| sumx | | sumy | sumxy | sumxsq | sumysq | | | |

Cell formulae

    y = (sig1-sig3)^2
    sigci = SQRT(sumy/n - (sumxy-sumx*sumy/n)/(sumxsq-(sumx^2)/n)*sumx/n)
    mi = (1/sigci)*((sumxy-sumx*sumy/n)/(sumxsq-(sumx^2)/n))
    r2 = ((sumxy-(sumx*sumy/n))^2)/((sumxsq-(sumx^2)/n)*(sumysq-(sumy^2)/n))

## APPENDIX C - CALCULATION OF MOHR-COULOMB PARAMETERS

The relationship between the normal and shear stresses can be expressed in terms of the corresponding principal effective stresses as suggested by Balmer [24]:

$$\sigma_n^{'} = \sigma_3^{'} + \frac{\sigma_1^{'} - \sigma_3^{'}}{\partial \sigma_1^{'}/\partial \sigma_3^{'} + 1} \qquad (C1)$$

$$\tau = (\sigma_1^{'} - \sigma_3^{'})\sqrt{\partial \sigma_1^{'}/\partial \sigma_3^{'}} \qquad (C2)$$

For the *GSI* > 25, when *a* = 0.5:

$$\frac{\partial \sigma_1^{'}}{\partial \sigma_3^{'}} = 1 + \frac{m_b \sigma_{ci}}{2(\sigma_1^{'} - \sigma_3^{'})} \qquad (C3)$$

For *GSI* < 25, when *s* = 0:

$$\frac{\partial \sigma_1'}{\partial \sigma_3'} = 1 + a m_b^a \left(\frac{\sigma_3'}{\sigma_{ci}}\right)^{a-1} \qquad (C4)$$

The tensile strength of the rock mass is calculated from:

$$\sigma_{tm} = \frac{\sigma_{ci}}{2}\left(m_b - \sqrt{m_b^2 + 4s}\right) \qquad (C5)$$

The equivalent Mohr envelope, defined by equation (4), may be written in the form:

$$Y = \log A + BX \qquad (C6)$$

where

$$Y = \log\frac{\tau}{\sigma_{ci}}, \quad X = \log\left(\frac{\sigma_n^{'} - \sigma_{tm}}{\sigma_{ci}}\right) \qquad (C7)$$

Using the value of $\sigma_{tm}$ calculated from equation (C5) and a range of values of $\tau$ and $\sigma_n^{'}$ calculated from equations (C1) and (C2), the values of *A* and *B* are determined by linear regression where :

$$B = \frac{\sum XY - (\sum X \sum Y)/T}{\sum X^2 - (\sum X)^2/T} \qquad (C8)$$

$$A = 10^\wedge\left(\sum Y/T - B\left(\sum X/T\right)\right) \qquad (C9)$$

and *T* is the total number of data pairs included in the regression analysis.

The most critical step in this process is the selection of the range of $\sigma_3'$ values. As far as the authors are aware, there are no theoretically correct methods for choosing this range and a trial and error method, based upon practical compromise, has been used for selecting the range included in the spreadsheet presented in Fig. C1.

For a Mohr envelope defined by equation (4), the friction angle $\phi_i^{'}$ for a specified normal stress $\sigma_{ni}^{'}$ is given by:

$$\phi_i^{'} = \arctan\left(AB\left(\frac{\sigma_{ni}^{'} - \sigma_{tm}}{\sigma_{ci}}\right)^{B-1}\right) \qquad (C10)$$

The corresponding cohesive strength $c_i^{'}$ is given by:

$$c_i^{'} = \tau - \sigma_{ni}^{'}\tan\phi_i^{'} \qquad (C11)$$

and the corresponding uniaxial compressive strength of the rock mass is :

$$\sigma_{cmi} = \frac{2c_i^{'}\cos\phi_i^{'}}{1 - \sin\phi_i^{'}} \qquad (C12)$$

Note that the cohesive strength $c_i^{'}$ given by equation (C11) is an upper bound value and that it is prudent to reduce this to about 75% of the calculated value for practical applications.

Fig. C1. Spreadsheet for calculation of Hoek-Brown and equivalent Mohr-Coulomb parameters

**Hoek-Brown and equivalent Mohr Coulomb failure criteria**

| **Input:** | sigci = | 85 | MPa | mi = | 10 | | GSI = | 45 |
|---|---|---|---|---|---|---|---|---|

| **Output:** | mb = | 1.40 | | s = | 0.0022 | | a = | 0.5 | |
|---|---|---|---|---|---|---|---|---|---|
| | sigtm = | -0.13 | MPa | A = | 0.50 | | B = | 0.70 | |
| | k = | 3.01 | | phi = | 30.12 | degrees | coh = | 3.27 | MPa |
| | sigcm = | 11.36 | MPa | E = | 6913.7 | MPa | | | |

| **Tangent:** | signt = | 15.97 | MPa | phit= | 30.12 | degrees | coht = | 4.12 | MPa |
|---|---|---|---|---|---|---|---|---|---|

**Calculation:**

| | | | | | | | | | Sums |
|---|---|---|---|---|---|---|---|---|---|
| sig3 | 1E-10 | 3.04 | 6.07 | 9.1 | 12.14 | 15.18 | 18.21 | 21.25 | 85.00 |
| sig1 | 4.00 | 22.48 | 33.27 | 42.30 | 50.40 | 57.91 | 64.98 | 71.74 | 347.08 |
| ds1ds3 | 15.89 | 4.07 | 3.19 | 2.80 | 2.56 | 2.40 | 2.27 | 2.18 | 35.35 |
| sign | 0.24 | 6.87 | 12.56 | 17.85 | 22.90 | 27.76 | 32.50 | 37.13 | 157.80 |
| tau | 0.94 | 7.74 | 11.59 | 14.62 | 17.20 | 19.48 | 21.54 | 23.44 | 116.55 |
| x | -2.36 | -1.08 | -0.83 | -0.67 | -0.57 | -0.48 | -0.42 | -0.36 | -6.77 |
| y | -1.95 | -1.04 | -0.87 | -0.76 | -0.69 | -0.64 | -0.60 | -0.56 | -7.11 |
| xy | 4.61 | 1.13 | 0.71 | 0.52 | 0.39 | 0.31 | 0.25 | 0.20 | 8.12 |
| xsq | 5.57 | 1.17 | 0.68 | 0.45 | 0.32 | 0.23 | 0.17 | 0.13 | 8.74 |
| sig3sig1 | 0.00 | 68.23 | 202.01 | 385.23 | 612.01 | 878.92 | 1183.65 | 1524.51 | 4855 |
| sig3sq | 0.00 | 9.22 | 36.86 | 82.94 | 147.45 | 230.39 | 331.76 | 451.56 | 1290 |
| taucalc | 0.96 | 7.48 | 11.33 | 14.45 | 17.18 | 19.64 | 21.91 | 24.04 | |
| sig1sig3fit | 11.36 | 20.51 | 29.66 | 38.81 | 47.96 | 57.11 | 66.26 | 75.42 | |
| signtaufit | 3.41 | 7.26 | 10.56 | 13.63 | 16.55 | 19.38 | 22.12 | 24.81 | |
| tangent | 4.253087 | 8.103211 | 11.40318 | 14.47286 | 17.3991 | 20.2235 | 22.97025 | 25.65501 | |

**Cell formulae:**

mb = mi*EXP((GSI-100)/28)

s = IF(GSI>25,EXP((GSI-100)/9),0)

a = IF(GSI>25,0.5,0.65-GSI/200)

sigtm = 0.5*sigci*(mb-SQRT(mb^2+4*s))

A = acalc = 10^(sumy/8 - bcalc*sumx/8)

B = bcalc = (sumxy - (sumx*sumy)/8)/(sumxsq - (sumx^2)/8)

k = (sumsig3sig1 - (sumsig3*sumsig1)/8)/(sumsig3sq-(sumsig3^2)/8)

phi = ASIN((k-1)/(k+1))*180/PI()

coh = sigcm/(2*SQRT(k))

sigcm = sumsig1/8 - k*sumsig3/8

E = IF(sigci>100,1000*10^((GSI-10)/40),SQRT(sigci/100)*1000*10^((GSI-10)/40))

phit = (ATAN(acalc*bcalc*((signt-sigtm)/sigci)^(bcalc-1)))*180/PI()

coht = acalc*sigci*((signt-sigtm)/sigci)^bcalc-signt*TAN(phit*PI()/180)

sig3 = Start at 1E-10 (to avoid zero errors) and increment in 7 steps of sigci/28 to 0.25*sigci

sig1 = sig3+sigci*(((mb*sig3)/sigci)+s)^a

ds1ds3 = IF(GSI>25,(1+(mb*sigci)/(2*(sig1-sig3))),1+(a*mb^a)*(sig3/sigci)^(a-1))

sign = sig3+(sig1-sig3)/(1+ds1ds3)

tau = (sign-sig3)*SQRT(ds1ds3)

x = LOG((sign-sigtm)/sigci)

y = LOG(tau/sigci)

xy = x*y          x sq = x^2          sig3sig1= sig3*sig1               sig3sq = sig3^2

taucalc = acalc*sigci*((sign-sigtm)/sigci)^bcalc

s3sifit = sigcm+k*sig3

sntaufit =  coh+sign*TAN(phi*PI()/180)

tangent = coht+sign*TAN(phit*PI()/180)